

article submitted to GRL, 12 August 2000; revised 16 October 2000

Mantle Flow at a Slab Edge: Seismic Anisotropy in the Kamchatka Region

Valerie Peyton,¹ Vadim Levin, Jeffrey Park, Mark Brandon, Jonathan Lees²
Yale University, New Haven, Connecticut

Evgenii Gordeev, Alexei Ozerov
Russian Academy of Sciences, Far Eastern Branch, Petropavlovsk-Kamchatsky

Abstract

The junction of the Aleutian Island and the Kamchatka peninsula defines a sharp turn in the boundary of the Pacific and North American plates, terminating the subduction zones of the northwest Pacific. The regional pattern of shear-wave birefringence near the junction indicates that trench-parallel strain follows the seismogenic Benioff zone, but rotates to trench-normal beyond the slab edge. Asthenospheric mantle is inferred to flow around and beneath the disrupted slab edge, and may influence the shallowing dip of the Benioff zone at the Aleutian junction.

Introduction

When oceanic lithosphere subducts into the mantle, it may undergo trench-axis rollback [Dewey, 1980; Otsuki, 1989], in which the asthenosphere under the slab is forced out of the way, either downward or along the trench towards the "free" end of the subduction zone. Trench-parallel mantle flow has been proposed for a variety of convergent settings [Alvarez, 1982; Giardini and Woodhouse, 1986; Russo and Silver, 1994; Yu and Park, 1994], and simulated in physical analog experiments [Buttles and Olson, 1998].

Kamchatka is one of the few places in the world where land-based observations can probe the upper mantle at and beyond the side edge of a mature subducting slab. A subduction zone underlies southern Kamchatka, terminating at the junction with the Aleutian Arc (Figure 1), where the Pacific plate boundary rotates into a transcurrent shear zone [Cormier, 1975]. Kamchatka and eastern Siberia constitute the western extremity of the North American Plate [Fujita *et al.*, 1990; DeMets, 1992; Kogan *et al.*, 2000], though some have argued for an Okhotsk subplate in the region [e.g., Riegel *et al.* 1993]. Rapid convergence (60–80 mm/yr) of the Pacific plate relative to North America is accommodated by subduction zones that flank the Aleutian, Kamchatka, and Kurile volcanic arcs. Both subduction and island-arc volcanism are interrupted by the strike-slip Bering fault zone along the western Aleutians (Komandorski Islands) [Geist and Scholl, 1994; Seliverstov, 1997]. The western Aleutians terminate against Cape Kamchatka at 56°N. The plate boundary extends southward as a convergent Benioff zone, but shallow historical seismicity also extends ~ 300 km northward [Fujita *et al.*, 1990], suggesting deformation complexity. Near the Kamchatka-Aleutian junction, the Kamchatka subduction zone lacks deep earthquakes, and Benioff-zone

dip decreases from 55° to 35° [Gorbatov *et al.*, 1997]. Magmatism shifts inland, following the shallowing slab. Present-day activity terminates in the vigorous Klyuchevskoy and Sheveluch volcanic centers.

This paper reports results of a collaborative study of the interaction of slab descent and asthenospheric flow under the Kamchatka peninsula. Lattice-preferred orientation (LPO) of olivine and orthopyroxene crystals in peridotite is thought to form by ductile flow in the upper mantle (150–400 km depth) [Christensen, 1984; Ribe, 1992; Zhang and Karato, 1995; Zhang *et al.*, 2000]. Olivine is highly anisotropic, and constitutes 40–60% of the mantle above 420 km depth. Therefore, mantle flow, both ongoing and fossil, is considered the cause of shear-wave birefringence in teleseismic body waves [Vinnik *et al.*, 1984; Silver and Chan, 1991] and Love-to-Rayleigh scattering in long-period surface waves [Yu and Park, 1994; Levin and Park, 1998]. These effects do not occur if the anisotropy has a near-vertical axis of symmetry, and so are useful indicators of lateral mantle flow.

SKS Splitting in Kamchatka

We deployed 15 portable broad-band seismic observatories in Kamchatka from Summer 1998 through Summer 1999. All stations were equipped with CMG-3T sensors and REF TEK data acquisition systems. Using GPS timing, we collected data continuously at 40 samples per second. Surf and cultural noise were problematic at several sites. We also used data from the station PET (Petropavlovsk-Kamchatsky) of the Global Seismographic Network. Figure 2 illustrates the distribution of events used in this report.

Figure 1 plots observations of shear wave splitting, performed on core-refracted shear phases discernible above the noise, typi-

cally after lowpassing at periods $T > 5$ s. At some stations (KRO, OSO) only waveforms lowpassed at $T > 10$ s were useful, due to surf noise. Many *SKS* observations involved phases arriving from the northeast (sources in Central and South America). Splitting observations at other backazimuths originated in the southern Pacific, central Atlantic and Indian Oceans (Figure 2). An electronic supplement file lists all observations of shear wave splitting for each station, with directions of approach and uncertainty estimates, performed using the cross-correlation technique described in *Levin et al.* [1999]. The small number of observations prevent us from interpreting backazimuth and incident-angle variations in splitting values, behavior that could resolve depth variation in anisotropic parameters [*Levin et al.*, 1999]. However, fast-polarization orientation is consistent within groups of adjacent stations, and the inferred orientation differences can be confirmed in simultaneous *SKS* waveforms from single events (Figure 3).

Shear-wave birefringence (splitting) parameters for *SKS* phases fall into two groups. Stations located above the active Benioff zone (APA, PET, KRO, MIL, TUM) exhibit a trench-parallel fast-polarization direction. Stations away from the slab show other fast-polarization orientations. Trench-normal directions at sites near the Kamchatka-Aleutian junction (ESS, KGB, BNG) rule out a strongly developed trench-parallel mantle fabric beyond the plate boundary corner, as might be expected in the case of strong trench-parallel flow. Trench-normal splitting at ESS, in particular, argues that the slab does not extend downdip beyond its seismogenic zone. This interpretation agrees with seismic tomography studies [*Gorbatov et al.*, 2000; *Lees et al.*, 2000] which report low seismic velocity beneath central Kamchatka. Only a handful of *SKS* phases exhibit split-

ting delay times $\delta t > 1$ s, and are mostly recorded at the northern stations. Typically, splitting delays $0.4 < \delta t < 0.8$ s, with formal uncertainties of 0.1–0.3 s, define the fast-polarization trends in Figure 2. Figure 3 shows a clear *SKS* phase simultaneously observed at stations TUM and ESS, yielding different birefringence parameters: trench-parallel fast-polarization and a delay of 0.44 sec at TUM; and trench-normal fast-polarization and a very small delay at ESS.

The splitting delay δt constrains the product of anisotropy and layer thickness. One must assume a level of anisotropy to estimate the thickness of the associated shear zone. If we assume 3% anisotropy with mean $V_s = 4.5$ km/s, corresponding to moderately strained upper mantle peridotite, a shear wave that traversed 90 km would accumulate $\delta t = 0.6$ s, consistent with a typical δt estimate from our data set.

Previous “source-side” estimates of mantle anisotropy near Kamchatka [*Kaneshima and Silver*, 1992; *Fischer and Yang*, 1994] were based on the differential splitting of teleseismic shear-phase pairs (e.g., S and sS) recorded at stations in North America. Our splitting delays δt are significantly smaller than the source-side estimates, which range between 1 and 2.35 s. Therefore the level and/or extent of anisotropic mantle beneath Kamchatka is less than indicated by earlier studies.

Discussion

Two lines of direct evidence support the notion that trench-parallel *SKS* splitting at APA, PET, KRO, MIL, and TUM originates below the Benioff zone: weak local- S splitting and the deformation of mantle xenoliths. S waves from earthquakes within the Kamchatka Benioff zone traverse the supra-slab mantle wedge and the crust and do not sample anisotropy within and be-

neath the slab. A group of such events exhibits only weak splitting at stations PET and APA (Figure 4). The observed local S fast-polarization axes vary greatly, the $\delta t = 0.1 - 0.3$ s are significantly smaller than the teleseismic splitting values at PET and APA, and the smallest splitting delays correspond to paths that are most vertical i.e., most representative of SKS raypaths. Similar weak splitting and irregular polarization in local S-waves for Kamchatka earthquakes was found by *Guseva et al.* [1991]. Mantle xenoliths found at Avachinsky Volcano near PET [Graybill et al., 1999] lack the kind of rock fabric that develops in a simple-shear flow. The xenoliths do not provide evidence for either a subduction-induced corner flow or a trench-parallel shear flow in the mantle wedge. We note that weak mantle-wedge fabric is consistent with other subduction-zone observations where back-arc spreading is weak [Fischer et al., 1998; Wiemer et al., 1999], and with the tank experiments of *Buttles and Olson* [1998].

We interpret the anisotropy implied by SKS splitting in terms of trench-parallel asthenospheric extension and/or flow beneath the Pacific plate. It is unlikely that the strain resides entirely in the slab itself, whether due to along-trench extension or fossil fabric. Present-day slab extension would not occur without strain in the adjoining asthenosphere. As for fossil slab fabric, an extrapolation of magnetic anomalies beyond the Cretaceous "quiet" magnetic zone predicts that the paleospreading direction within the slab under Kamchatka should be near-normal to the trench.

The anisotropic fast-polarization directions for stations that border the shallow seismogenic zone are trench-normal, suggesting strain and/or mantle flow across the plate boundary. Splitting at BNG is likely influenced by the distributed transcurrent deformation along the western Aleu-

tians [Cormier, 1975; Geist and Scholl, 1994]. Splitting at KGB and ESS argues for flow around and beneath the tattered slab edge. North of the Aleutian junction along an extinct subduction zone bordering the Bering Sea [Seliverstov, 1997], splitting at PAN, OSO and TKI is larger and scattered, but inconsistent with any trench-parallel flow. Though 1.3 Ma volcanic rocks have been reported in the region [Honthaas et al. 1995], *Hochstaedler et al.* [1994] argue from geochemical evidence that subduction in northern Kamchatka had weakened or halted during the eruption of the Valovayam volcanic field near OSO at 6–8 Ma.

Trench-normal fast-polarization near the Kamchatka-Aleutian corner could indicate the shearing of asthenosphere as the slab falls through it. Trench-axis regression would also induce asthenospheric flow from the Pacific to the North American side of the plate boundary. If trench regression occurs, it is likely smaller than in locales where back-arc spreading is vigorous, such as the Lau Basin and the Phillipine Sea. However, the Sea of Okhotsk is thought to be underlain by extended continental lithosphere [Gnibidenko and Khvedchuk, 1982; Melankholina, 1998], and a central graben divides southern Kamchatka into eastern and western mountain ranges. Weaker slab migration may be consistent with the small SKS splitting delays we observe in Kamchatka.

In tank experiments to simulate the regression of a dipping slab through the mantle, *Buttles and Olson* [1998] observed significant displacement of asthenosphere beneath the slab as well as around it laterally. Beneath Kamchatka, where *Davaille and Lees* [2000] argue that the slab edge may have been lost through small-scale convective instability, such "pass-through" flow is likely (Figure 5). The change in Benioff-zone dip near the Aleutian corner could be facilitated by the loss of the downdip load

and a lofting of the plate edge by mantle flow beneath it. A consequent shallowing of the plate edge and the supra-slab mantle would induce pressure-release volcanism, and could be partly responsible for the voluminous Klyuchevshoy volcanism, the inferred contribution of “adakite” slab-derived melts to Sheveluch volcanism [Kepezhinskas *et al* 1997; Yagodinski *et al* 2000], and the widening of the central Kamchatka graben opposite the plate corner.

Acknowledgments. Comments from two anonymous reviewers helped to clarify some points. This research was supported by the NSF grant EAR-9614639. The resourcefulness of the Kamchatka Experimental-Methodical Seismic Department (V. Chebrov, O. Dontsov, E. Tokarev, V. Stepanov, V. Sinitsyn, N. Titkov, I. Semchenko) and support from the Institute of Volcanology (V. Gorelichik, A. Osipenko, L. Osipenko) was critical to the success of the field campaign. Creative cargo handling by Reeve Aleutian Airlines is appreciated. We used PASSCAL seismic equipment from the Incorporated Research Institutions for Seismology. Matthew Fouch, Paul Friberg, Noel Barstow and Doug Johnson of PASSCAL all helped this project succeed. We used **GMT** software [Wessel and Smith, 1991] to prepare figures.

References

- Alvarez, W., Geological evidence for the geographical pattern of mantle return flow and the driving mechanism of plate tectonics, *J. Geophys. Res.*, *87*, 6697–6710, 1982.
- Buttles, J. and P. Olson, A laboratory model of subduction zone anisotropy, *Earth Planet. Sci. Lett.*, *164*, 245–262, 1998.
- Christensen, N. I., The magnitude, symmetry and origin of upper mantle anisotropy from fabric analyses of ultramafic tectonites, *Geophys. J. R. Astron. Soc.*, *76*, 89–111, 1984.
- Cormier, V. F., Tectonics near the junction of the Aleutian and Kuril-Kamchatka arcs and a mechanism for middle Tertiary magmatism in the Kamchatka basin, *Geol. Soc. Am. Bull.*, *86*, 443–453, 1975.
- Davaille, A., and J. M. Lees, Thermal modeling in torn, subducted plate edges *Geophys. Res. Lett.*, submitted 2000.
- DeMets, C., A test of present-day plate geometries for northeast Asia and Japan, *J. Geophys. Res.*, *97*, 17627–17635, 1992.
- Dewey, J. F., Episodicity, sequence, and style at convergent plate boundaries, in *The Continental Crust and its Mineral Deposits*, D. W. Strangway, ed., *Geol. Assoc. Can., Spec. Pap.*, *20*, 553–573, 1980.
- Fischer, K. M. and X. Yang, Anisotropy in Kuril-Kamchatka subduction zone structure, *Geophys. Res. Lett.*, *21*, 5–8, 1994.
- Fischer, K. M., M. Fouch, D. Wiens and M. Boettcher, Anisotropy and flow in Pacific subduction zone back-arcs, *Pure Appl. Geophys.*, *151*, 463–475, 1998.
- Fujita, K., D. B. Cook, H. Gasegawa, D. Forsyth and R. Wetmiller, Seismicity and focal mechanisms of the Arctic region and the North American plate boundary in Asia, in *The Arctic Ocean Region (The Geology of North America)*, A. Grantz, L. Johnson and J. F. Sweeney (Editors) Geological Society of America, Boulder, 1990.
- Geist, E. L. and D. W. Scholl, Large-scale deformation related to the collision of the Aleutian arc with Kamchatka, *Tectonics*, *13*, 538–560, 1994.
- Giardini, D. and J. H. Woodhouse, Horizontal shear flow in the mantle beneath Tonga arc, *Nature*, *319*, 551–555, 1986.
- Gnibidenko, H. S., and I. I. Khvedchuk, The tectonics of the Okhotsk Sea, *Mar. Geol.*, *50*, 155–198, 1982.
- Gorbatov, A., V. Kostaglodov, G. Suarez, and E. Gordeev, Seismicity and structure of the Kamchatka subduction zone, *J. Geophys. Res.*, *102*, 17883–17898, 1997.
- Gorbatov, A., A. Widiyantoro, Y. Fukao, and E. Gordeev, Signature of remnant slabs in the North Pacific from *P*-wave tomography, *Geophys. J. Int.*, *142*, 27–36, 2000.

- Graybill, J., M. T. Brandon, and P. K. Kepezhinskas, Olivine lattice-preferred orientation in xenoliths from the mantle wedge beneath the Southern Kamchatka volcanic arc (abstract), *Eos Trans. AGU*, 80, F926, 1999.
- Guseva, E. M., A. A. Gusev, and L. S. Osborn. A software package for earthquake data processing: experimental application to strong motion record. *Volcanology and Seismology*, 11, 648-670, 1991.
- Hochstaedler, A. G., P. K. Kepezhinskas, M. J. Defant, M. S. Drummond, and H. Bellon, On the tectonic significance of arc volcanism in northern Kamchatka, *J. Geology*, 102, 639-654, 1994.
- Honthaas, C., Bellon, H., Kepezhinskas, P. K., and R. C. Maury, New ^{40}K - ^{40}Ar dates for the Cretaceous-Quaternary magmatism of Northern Kamchatka (Russia), *C. R. Acad. Sci. Paris, Serie II*, 320, 197-204.
- Kaneshima, S., and P. G. Silver, A search for source-side anisotropy, *Geophys. Res. Lett.*, 19, 1049-1052, 1992.
- Kepezhinskas, P. K., F. McDermott, M. J. Defant, A. Hochstaedler, M. S. Drummond, C. J. Hawkesworth, A. Koloskov, R. C. Maury, and H. Bellon, Trace element and Sr-Nd-Pb isotopic constraints on a three-component model of Kamchatka Arc petrogenesis, *Geochim. Cosmochim. Acta*, 61, 577-600, 1997.
- Kogan, M. G., G. M. Steblov, R. W. King, T. A. Herring, D. I. Frolov, S. G. Egorov, V. Ye. Levin, A. Lerner-Lam, and A. Jones, Geodetic constraints on the rigidity and relative motion of Eurasia and North America, *Geophys. Res. Lett.*, 27, 2041-2044, 2000.
- Lees, J. M., J. Vandecar, E. Gordeev, A. Ozerov, V. Peyton, J. Park, V. Levin and M. T. Brandon, Tomographic images of the Kamchatka slab, to be submitted to *Science*, 2000.
- Levin, V., and J. Park, Quasi-Love phases between Tonga and Hawaii: observations, simulations and explanations, *J. Geophys. Res.*, 103, 24321-24331, 1998.
- Levin, V., W. Menke and J. Park, Shear wave splitting in Appalachians and Urals: a case for multilayered anisotropy, *J. Geophys. Res.*, 104, 17975-17994, 1999.
- Melankholina, E. N., The types of back-arc basins in East Asia: Tectonic, magmatic, and geodynamic aspects, *Geotectonics*, 32, 453-467, 1998.
- Otsuki, K., Empirical relationships among the convergence rate of plates, rollback rate of trench axis and island-arc tectonics: "Laws of the convergence of plates," *Tectonophysics*, 159, 73-94, 1989.
- Ribe, N. M., On the relationship between seismic anisotropy and finite strain, *J. Geophys. Res.*, 97, 8737-8748, 1992.
- Riegel, S. A., Fujita, K., Koz'min, B. M., Imaev, V. S., and D. B. Cook, Extrusion tectonics of the Okhotsk Plate, northeast Asia, *Geophys. Res. Lett.*, 20, 607-610, 1993.
- Russo, R. M. and P. G. Silver, Trench-parallel flow beneath the Nazca Plate from seismic anisotropy, *Science*, 263, 1105-1111, 1994.
- Seliverstov N. I., Geodynamic evolution of the junction zone of the Kuril-Kamchatka and Aleutian island arcs (in Russian), *Vulkanologiya i Seysmologiya*, 3, 12-17, 1997.
- Silver, P. G., and W. W. Chan, Shear-wave splitting and subcontinental mantle deformation, *J. Geophys. Res.*, 96, 16429-16454, 1991.
- Vinnik, L. P., Kosarev, G. L., and Makeyeva L. I., Anisotropy of the lithosphere according to the observations of *SKS* and *SKKS* waves (in Russian), *Doklady Akademii Nauk SSSR*, 278, 1335-1339, 1984.
- Weimer, S., G. Tytgat, M. Wyss, and U. Duenkel, Evidence for shear-wave anisotropy in the mantle wedge beneath south-central Alaska, *Bull. Seismol. Soc. Am.*, 89, 1313-1322, 1999.
- Wessel, P., and W. H. F. Smith, Free software helps map and display data, *Eos Trans. AGU*, 72, 441, 1991.
- Yogodzinski, G. M., J. M. Lees, T. G. Churikova, F. Dorendorf, and O. N. Volynets,

Slab edge effects on arc magma geochemistry: Evidence of a torn Pacific plate beneath Kamchatka and the western Aleutians, *Nature*, accepted 2000.

Yu, Y., and J. Park, Hunting for azimuthal anisotropy beneath the Pacific Ocean region, *J. Geophys. Res.*, *99*, 15399–15421, 1994.

Zhang, S., and S.-I. Karato, Lattice preferred orientation of olivine aggregates deformed in simple shear, *Nature*, *375*, 774–777, 1995.

Zhang, S., S.-I. Karato, J. FitzGerald, U. H. Faul, and Y. Zhou, Simple shear deformation of olivine aggregates, *Tectonophysics*, *316*, 133–152, 2000.

Valerie Peyton, U.S. Geological Survey, Seismological Laboratory, Building 10002, Kirtland AFB-East, Albuquerque, NM 87115, valerie@asl.cr.usgs.gov

Vadim Levin, Jeffrey Park, and Mark Brandon, Dept. of Geology and Geophysics, Box 208109, Yale Univ., New Haven, CT 06520, USA, [vadim, park, brandon]@geology.yale.edu

Jonathan Lees, Department of Geological Sciences, Campus Box 3315, Mitchell Hall, Univ. of North Carolina, Chapel Hill, NC 27599-3315, USA, jonathan.lees@unc.edu

Evgenii Gordeev and Alexei Ozerov, Russian Academy of Sciences, Far Eastern Branch, Petropavlovsk-Kamchatsky, Russia, [gord, ozerov]@emsd.iks.ru

Received ; revised ; accepted .

¹Now at U.S. Geological Survey, Albuquerque, New Mexico.

²Now at University of North Carolina, Chapel Hill.

This preprint was prepared with AGU's L^AT_EX macros v5.01. File sks-grl formatted October 25, 2000.

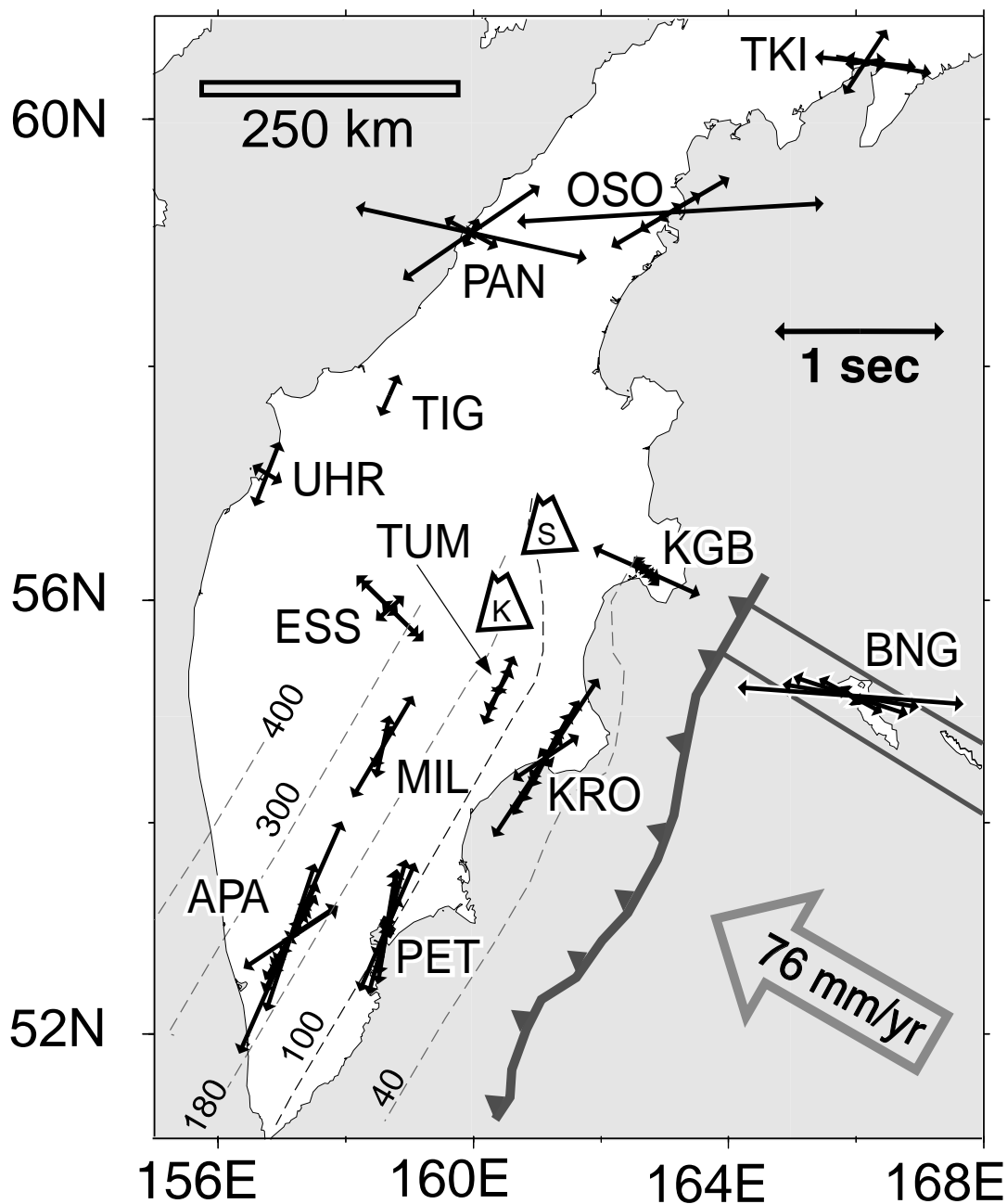


Figure 1. Shear-wave splitting observations at permanent seismological station PET and a portable broadband seismic network in Kamchatka region. Arrows represent single-record birefringence observations. The contours of the Benioff zone under Kamchatka are adapted from *Gorbatov et al.* [1997]. Thick gray arrow shows direction of the Pacific plate motion (subduction along the Kamchatka trench and transcurrent motion along Bering Fault). The transcurrent boundary, distributed across the overriding North American plate [*Geist and Scholl, 1994*], is indicated by two thin grey lines. Two volcanoes are marked on the map: *K* - Klyuchevskoy; *S* - Sheveluch.

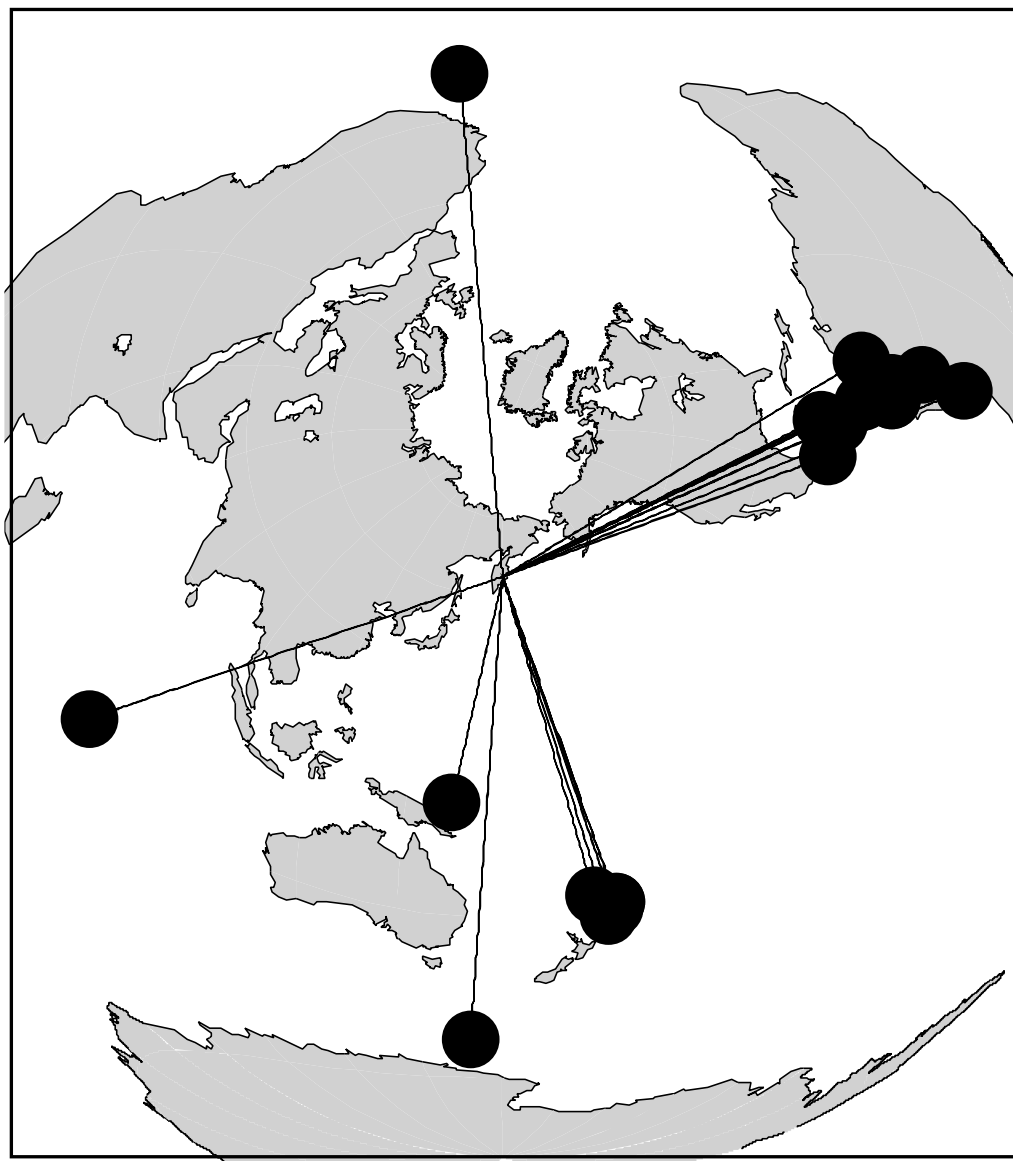


Figure 2. Earthquakes used as sources for the study of *SKS* splitting in Kamchatka.

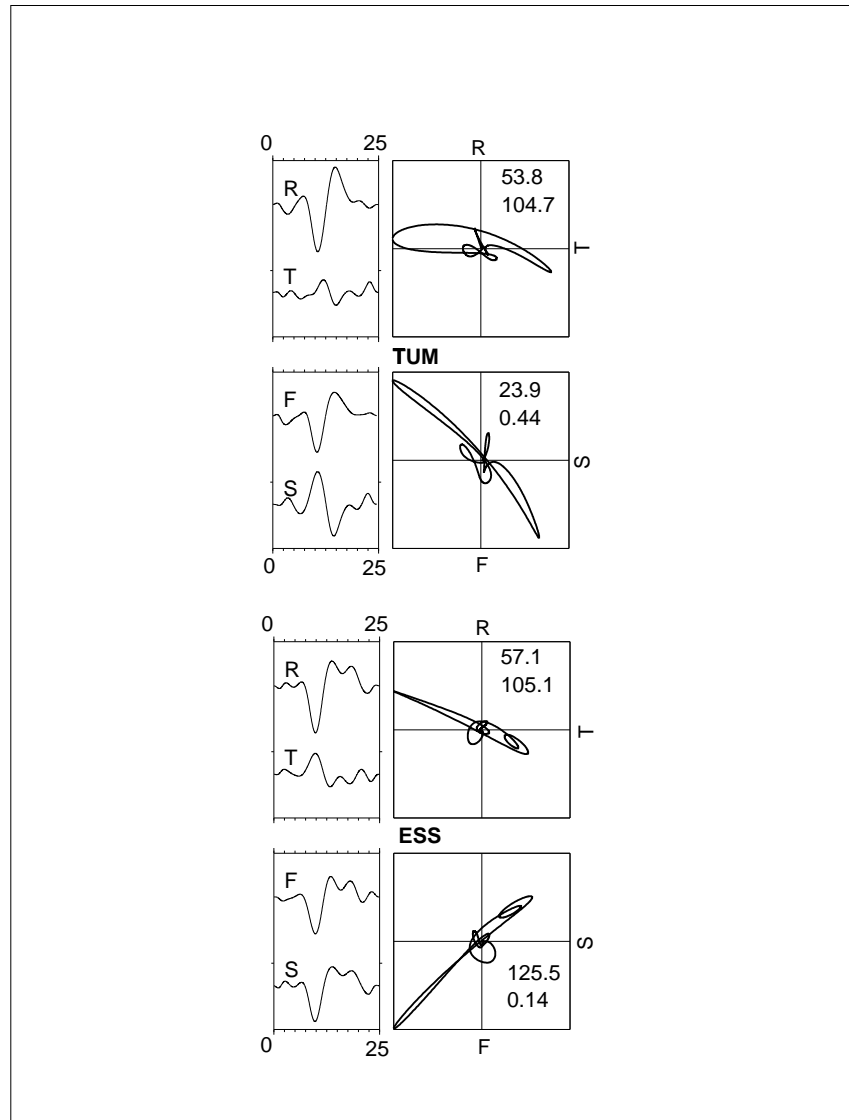


Figure 3. Shear wave splitting examples for stations TUM (top four panels) and ESS (bottom four panels). For each station, the upper left panel graphs the horizontal waveforms of the observed shear phase, rotated into the radial-transverse coordinate frame. Birefringence in the waveform is manifested by ellipticity of the particle motion (upper right panel). The numbers in the particle-motion box are back-azimuth and epicentral distance, in degrees. For each station, the lower left panel graphs the waveforms rotated into the fast and slow polarizations, with the slow component advanced by the estimated splitting delay. The lower right panel graphs corrected near-rectilinear particle motion. The numbers in the particle motion box are fast-polarization azimuth in degrees and time delay between fast and slow components in seconds.

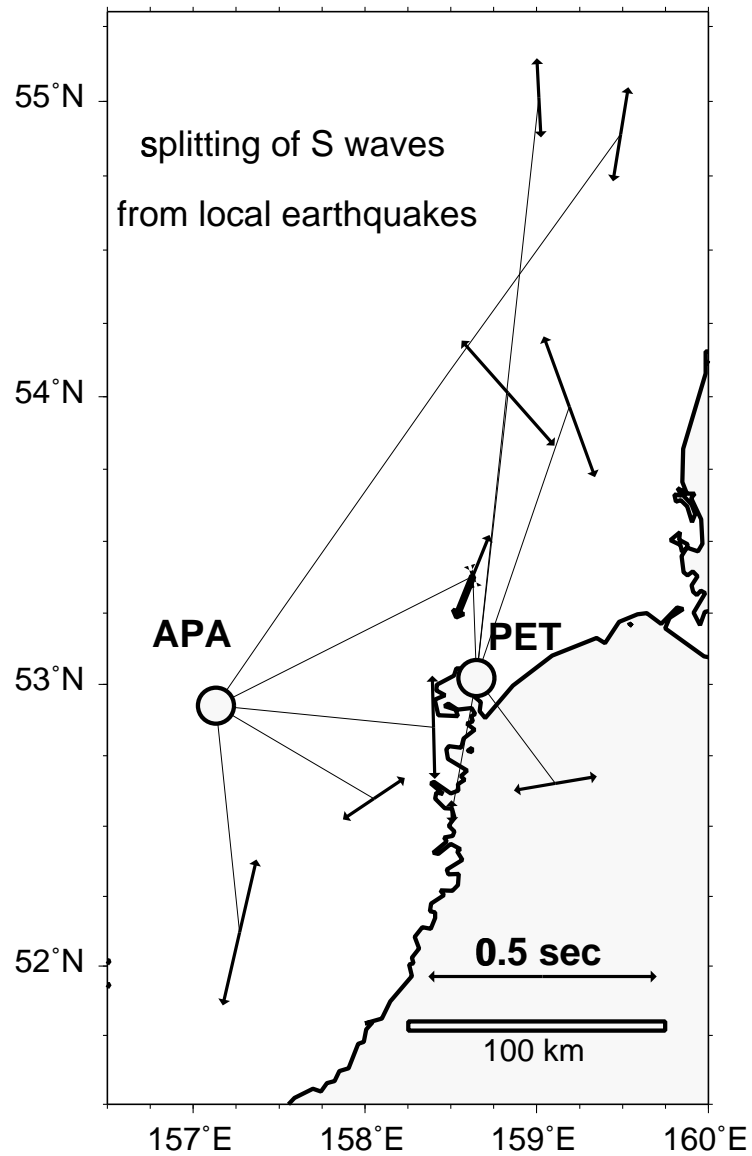


Figure 4. Shear-wave splitting observations from local S waves at stations APA and PET. Arrows represent single-record birefringence observations, placed at the epicenter of earthquakes in the Kamchatka subduction zone. Locations are from the reviewed catalog of the Kamchatka Experimental-Methodical Seismic Department (Russian acronym KOMSP). Note the scale difference for splitting delay δt relative to Figure 1.

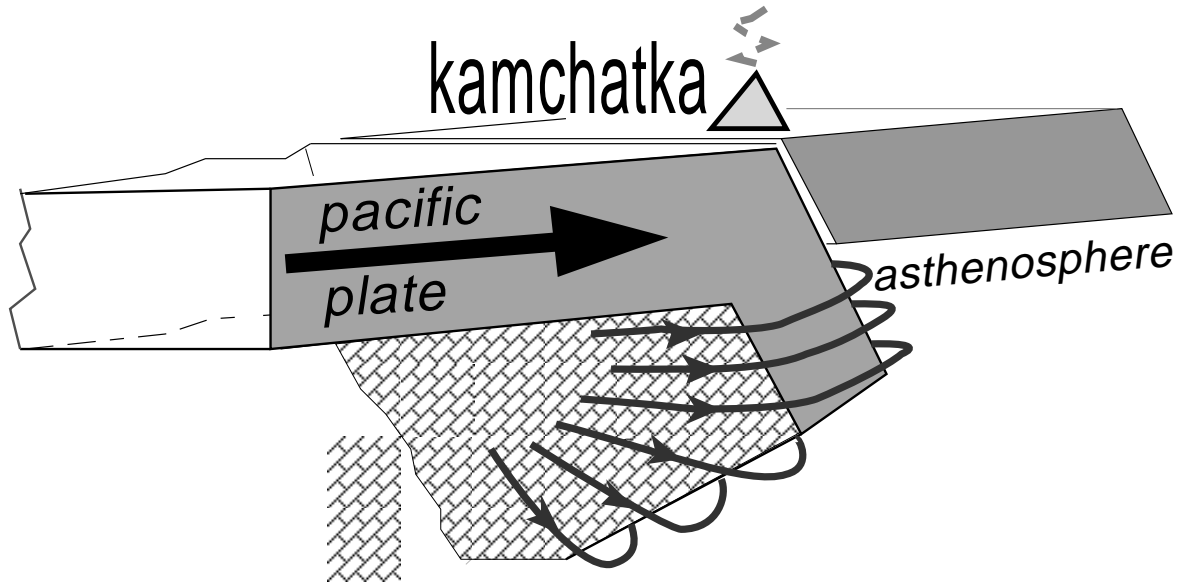


Figure 5. Schematic diagram for slab-edge mantle flow suggested by shear-wave splitting observations from portable seismic network in Kamchatka. Mantle extension is trench-parallel beneath the slab itself, driven by asthenospheric flow as the slab descends and retreats from the Eurasian landmass. At stations above the slab, shear-wave splitting is trench-parallel. Near the tattered slab edge, asthenosphere flows from beneath the Pacific Plate to beneath the overriding plate. Here the olivine LPO aligns its fast axis with the flow to become trench-normal.

Table 1. ELECTRONIC SUPPLEMENT: Splitting measurements shown in Figure 1. Details of the measurement technique are in *Levin et al, J. Geophys. Res., , 104, 17975–17994, 1999*. Code is available from W. Menke's website at LDEO. Fields in the table: sta- station name backazi - backazimuth to the event, CW from NORTH, in degrees direction - estimate of the fast shear wave propagation direction, CCW from EAST, in degrees delay - time lag between fast and slow components dir err, delay err - errors of the above two values C - crosscorrelation coefficient of the two components snr1, snr2, over - estimates of signal/noise ratio (two methods) and oversampling parameter, used in deriving error bounds. event - event tag (YYYY.JJ.JJ.MM)

sta	backazi	fast dir	delay	dir err	delay err	C	snr1	snr2	over	event
APA	182.15	33.45	0.68	6.14	0.33	0.91	3.10	2.38	56.	1998.181.00.01
APA	63.42	62.04	0.23	5.85	0.35	0.91	3.24	2.74	69.	1998.216.19.23
APA	63.15	58.36	0.42	14.32	0.08	0.99	9.32	4.51	45.	1998.235.14.20
APA	247.93	66.22	1.54	11.67	0.30	0.92	3.35	2.39	73.	1999.024.08.24
APA	56.44	71.66	0.94	7.77	0.19	0.94	3.84	2.42	38.	1999.025.18.43
APA	61.78	57.99	0.35	7.64	0.20	0.94	4.07	3.53	78.	1999.090.06.18
APA	66.34	64.24	0.74	9.17	0.19	0.95	4.32	2.88	48.	1999.093.06.42
APA	66.99	59.16	0.60	10.83	0.24	0.87	2.53	1.80	46.	1999.125.23.03
APA	61.12	64.97	0.49	11.95	0.10	0.99	12.42	7.24	67.	1999.192.14.36
APA	157.84	73.25	0.04	11.50	0.17	0.95	4.31	3.00	51.	1999.209.00.38
BNG	70.57	135.98	0.16	10.11	0.09	0.97	5.42	8.18	66.	1998.216.19.22
BNG	68.98	170.41	0.83	13.79	0.28	0.94	4.00	2.88	67.	1999.090.06.17
BNG	73.29	151.76	0.43	9.27	0.14	0.96	4.67	3.23	43.	1999.093.06.41
BNG	68.88	175.74	1.37	13.30	0.28	0.96	4.20	2.45	73.	1999.116.18.40
BNG	68.29	142.56	0.18	11.86	0.16	0.96	5.19	3.02	62.	1999.192.14.36
BNG	166.20	161.74	0.73	7.91	0.22	0.67	1.42	1.57	37.	1999.209.10.30
ESS	57.12	140.62	0.13	10.50	0.05	0.99	9.37	6.77	36.	1999.025.18.43
ESS	62.59	135.40	0.56	7.60	0.15	0.87	2.61	2.39	41.	1999.090.06.18
ESS	65.88	41.30	0.22	7.59	0.21	0.93	3.60	2.84	51.	1999.093.06.42
ESS	162.47	135.34	0.48	15.59	0.18	0.96	5.02	2.85	34.	1999.099.12.35
KGB	66.04	75.85	0.05	13.06	0.31	0.94	4.13	2.75	107.	1999.090.06.17
KGB	69.58	155.88	0.71	7.84	0.14	0.93	3.68	3.26	54.	1999.093.06.41
KGB	166.05	130.30	0.11	8.94	0.09	0.91	3.12	2.51	24.	1999.099.12.35
KGB	164.58	47.77	0.05	8.01	0.08	0.96	4.74	3.05	25.	1999.110.19.26
KGB	65.67	145.86	0.19	12.96	0.19	0.98	6.78	3.47	77.	1999.116.18.40
KGB	163.43	130.37	0.23	10.80	0.15	0.96	5.22	3.42	61.	1999.209.10.30
KRO	66.35	63.34	0.40	11.64	0.06	0.99	10.38	5.83	42.	1998.235.14.19
KRO	59.62	59.85	0.80	12.51	0.33	0.81	2.04	2.01	102.	1999.025.18.42
KRO	64.93	33.84	0.48	10.44	0.47	0.75	1.71	1.71	82.	1999.090.06.18
KRO	69.10	56.55	1.15	15.22	0.70	0.86	2.43	1.99	193.	1999.093.06.41
KRO	64.74	61.21	0.61	9.81	0.24	0.93	3.75	2.72	65.	1999.116.18.40
KRO	64.35	52.78	0.31	16.22	0.06	0.95	4.16	4.61	24.	1999.192.14.36
KRO	162.07	121.55	0.14	9.97	0.13	0.91	3.23	2.75	45.	1999.209.10.30
MIL	57.31	77.66	0.39	8.31	0.12	0.98	6.83	5.40	65.	1999.025.18.43
MIL	62.71	67.02	0.27	9.29	0.08	0.99	9.75	6.13	57.	1999.090.06.18
MIL	62.39	59.38	0.71	7.91	0.24	0.90	3.06	2.73	59.	1999.116.18.40
OSO	60.45	3.40	1.85	17.24	1.17	0.96	5.18	0.72	67.	1999.025.18.42
OSO	163.13	30.43	0.83	14.31	0.26	0.86	2.47	2.14	108.	1999.200.02.39
OSO	163.06	30.79	0.43	14.14	0.11	0.96	4.71	2.71	38.	1999.209.00.39
OSO	163.61	33.47	0.18	7.39	0.09	0.92	3.49	3.50	37.	1999.213.09.01
PAN	57.63	62.88	0.19	15.60	0.29	0.97	5.71	3.32	100.	1999.025.18.42
PAN	63.25	151.56	0.37	8.76	0.10	0.98	6.52	5.56	64.	1999.090.06.17
PAN	65.21	59.49	0.05	11.25	0.09	0.99	8.86	5.05	44.	1999.093.06.41
PAN	162.27	34.46	1.00	12.74	0.34	0.98	6.39	2.54	48.	1999.110.19.26
PAN	61.96	167.50	1.43	12.49	0.60	0.84	2.29	2.13	83.	1999.240.13.03
TIG	56.71	66.15	0.27	7.29	0.09	0.96	5.30	4.76	37.	1999.025.18.42
TKI	63.04	170.18	0.80	12.35	0.22	0.90	3.06	2.13	49.	1999.025.18.42
TKI	169.19	167.63	0.25	15.23	0.09	0.98	6.31	3.28	35.	1999.099.12.36
TKI	167.44	6.05	0.24	9.85	0.04	0.98	7.38	7.02	23.	1999.110.19.26
TKI	67.72	174.15	0.61	13.98	0.23	0.97	5.42	3.10	98.	1999.116.18.40
TKI	166.36	56.84	0.46	10.10	0.19	0.90	3.03	2.52	59.	1999.209.10.30
TUM	58.83	66.23	0.46	8.80	0.07	0.98	7.59	5.51	40.	1999.025.18.42
TUM	63.89	61.20	0.30	8.56	0.21	0.94	4.09	3.17	55.	1999.116.18.41
TUM	63.77	81.30	0.07	27.58	0.10	0.98	7.43	2.79	40.	1999.192.14.36
UHR	158.41	68.70	0.42	8.42	0.20	0.88	2.67	2.60	57.	1999.209.10.30
UHR	59.55	149.70	0.21	8.23	0.30	0.84	2.28	2.26	86.	1999.240.13.03
PET	63.60	80.53	0.70	11.91	0.22	0.96	4.64	3.23	37.	1998.093.22.25
PET	352.75	107.05	0.15	9.69	0.48	0.82	2.15	2.07	56.	1998.100.17.05
PET	64.74	67.49	0.39	9.02	0.20	0.95	4.20	4.33	31.	1998.216.19.23
PET	64.38	84.03	0.02	11.47	0.05	0.99	11.48	6.65	23.	1998.235.14.19
PET	57.78	79.41	0.59	14.00	0.09	0.99	17.50	8.67	39.	1999.025.18.43
PET	63.07	80.72	0.09	10.14	0.05	0.99	18.22	11.22	30.	1999.090.06.18
PET	67.75	74.40	0.85	11.66	0.24	0.96	5.12	3.68	52.	1999.093.06.42
PET	63.01	66.63	0.85	20.70	0.32	0.97	6.11	2.45	42.	1999.116.18.41

Table 2. ELECTRONIC SUPPLEMENT: Locations of earthquakes used in the analysis.

Lat	Lon	Event
-60.35	153.14	1998.181.00
-0.59	-80.39	1998.216.19
11.66	-88.04	1998.235.14
-26.46	74.48	1999.024.08
4.46	-75.72	1999.025.18
5.83	-82.62	1999.090.06
-16.66	-72.66	1999.093.06
-26.35	178.22	1999.099.12
-31.89	-179.04	1999.110.19
-1.65	-77.78	1999.116.18
14.36	-94.67	1999.125.23
15.78	-88.33	1999.192.14
-28.63	-177.61	1999.200.02
-28.69	-177.52	1999.209.00
-178.01	-30.29	1999.209.10
-30.37	-177.83	1999.213.09
-1.29	-77.55	1999.240.13
-8.15	-74.24	1998.093.22
-1.32	-15.65	1998.100.17
-0.59	-80.39	1998.216.19